10.21611/qirt.2020.015

15th Quantitative InfraRed Thermography Conference

Neural network based automated defect detection using induction thermography for surface cracks of forged parts

by D. Müller[1,2], U. Netzelmann[1], A. Ehlen[1,2], M. Finckbohner[1] and B. Valeske[1,2]

[1] Fraunhofer Institute for Nondestructive Testing IZFP, Campus E3 1, 66123 Saarbrücken, Germany,
[2] Hochschule für Technik und Wirtschaft des Saarlandes, htw saar, Goebenstr. 40, 66117 Saarbrücken, Germany, david.mueller@izfp.fraunhofer.de

Abstract

A fully convolutional neural network was set up for the detection of crack-type defects and for the defect shape prediction of thermography datasets. The method uses a supervised neural network for sematic segmentation (U-Net). For these tasks, training datasets of forged parts were acquired through induction thermography. The approach provides a significant improvement over conventional methods of thermal signal and image processing used in active thermography. Furthermore, the results may lead to new procedures for a quantitative evaluation of flaws and defects in non-destructive testing using infrared thermography.

Introduction

Induction thermography could be applied in many industrial sectors, where forged steel components are used, e.g. automotive industry, aerospace industry or water supply (steel water pipes). Despite constant improvements in the manufacturing processes, defects can occur in the manufactured components. For this reason, non-destructive testing of the components, such as ultrasound testing (UT) for volume defects and magnetic particle testing (MT) for surface defects, is generally required. Fully automated testing using induction thermography attempts to achieve at least the same high level of testing reliability as the established method, with at least the same, but ideally shorter testing times. Customers demand a fast non-destructive methodology that assesses whether the part to be tested is free of defects. Induction thermography is already used industrially to detect cracks in bar material [1] and in small components [2]. The technology was also applied to parts and components, mainly made of steel [3,4]. At Fraunhofer IZFP, validation studies for induction thermography were carried out to determine the detection limits for crack-like surface defects [5]. Further work demonstrated the detectability of hidden defects up to a depth of about 1 mm in ferritic steel [6], which is normally not possible with MT. Using inductive excitation, the integrity of bonded joints in the automotive sector was investigated [7]. Current research by Oswald-Tranta et al. is concerned with determining the crack depth from the cooling sequences of thermography [8]. The focus of this work is the improved automatic crack detection in induction thermography. Therefore, we choose a neural network approach for semantic segmentation known from medical technology and the automotive industry. In 2015, Ronneberger et al. introduced a U-shaped network for segmentation of cancer tumours of nuclei, also known as U-Net [9]. Through data augmentation, this network can be trained end-to-end from very few images. The U-Net can be applied to thermographic problems and is used in this work for improved defect detection in forged parts.

Principle of the method

Induction (or pulsed eddy current) thermography uses electromagnetic pulses to initially excite eddy currents in electrically conductive materials. For this purpose, an inductor is positioned at a small distance from the component surface to be inspected for surface defects. High-frequency currents induce eddy currents in the component surface in the form of closed current loops. The current paths in the test object are disturbed by surface defects. If the induced current hits a surface crack, it must take a detour around the crack. The flow of current in the component is associated with heating due to ohmic losses. At cracks, the current density is changed and a characteristic defect signature becomes visible to an infrared camera. Figure 1 shows the schematic measurement setup for induction thermographic examination of a forged part.

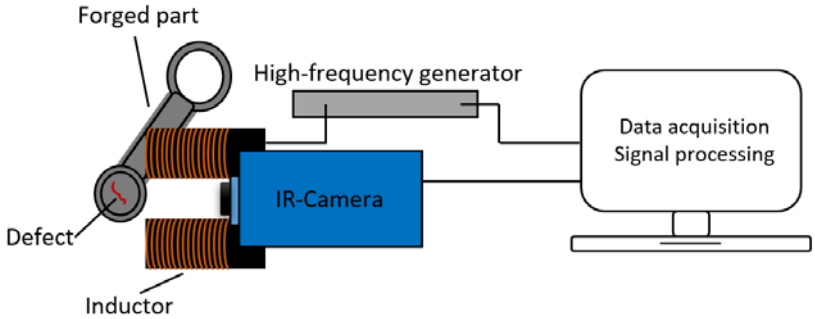

Fig. 1. *Scheme of the induction thermography measurement setup*

The raw image sequence already reveals the defect indications searched for. However, defects are often still overlaid by reflections of interfering radiation on the test object surface and inhomogeneities due to lift-off effects and emissivity fluctuations. Forged parts are often geometrically complex and can vary in size. It is therefore necessary to examine them in different sub-areas. The use of the infrared camera makes it possible to react flexibly to different part geometries and to inspect a component at different locations with the support of a robot. Since the MT images were already available at the beginning of the work, an area was selected for this work where the probability of defect appearance was the highest (figure 2).

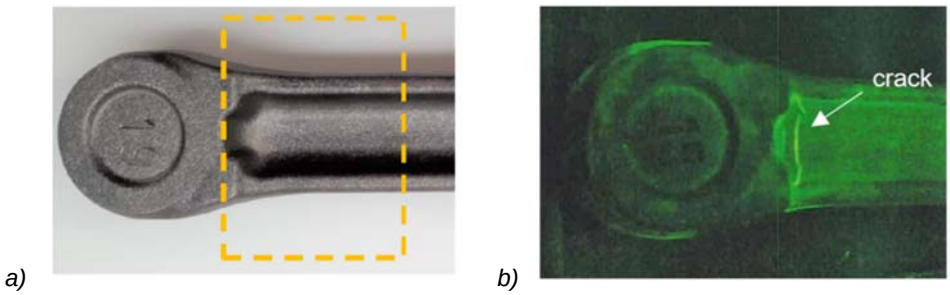

Fig. 2. *a) Example of one of the examined forged part with the area to be examined. b) MT image provided by the manufacturer with clearly visible crack indication.*

In total, 44 forged parts sorted out from the running production with different fine surface cracks were examined. Measurement data were acquired with a FLIR SC5200 mid-wave IR camera. The sampling rate was 320 Hz. As pre-processing, pulsed-phase thermography (PPT) was calculated for the recorded image sequence. To preprocess the data, the pulsed-phase transformation was performed [10]. The time dependence of the images was transformed into the frequency space for each pixel by

$$F_n = \sum_{k=0}^{N-1} T_k e^{\frac{-2\pi i k n}{N}} = Re_n + Im_n \qquad (1)$$

The amplitude A_n (eq.2) and phase φ_n (eq.3) can be then calculated from the real and imaginary parts of the transformation result for each analysis frequency by

$$A_n = \sqrt{{Re_n}^2 + {Im_n}^2} \qquad (2)$$

$$\varphi_n = arctan\frac{Im_n}{Re_n} \qquad (3)$$

The strength of the phase images is that they ideally represent only time-dependent effects and that multiplicative influences such as inhomogeneous excitation and heating as well as local variations in infrared emissivity are suppressed. Automatic defect detection is performed by using the U-Net network architecture. The U-Net works on the basis of convolutional networks for semantic segmentation. The underlying principle is that of an encoder/decoder structure: the spatial resolution of the input image is down-sampled and low-resolution feature mappings are generated. Low-resolution mappings are generated by different convolutional layers with different filtering aspects. In order to get a comprehensive overview, the full concept of U-Net has been thoroughly described in [9]. As input for the U-Net, only phase images at the lowest meaningful frequency were chosen. For this input data set, corresponding binary masks were created, which were assigned to the network as output data. In this implementation of the NN, each pixel is assigned to a binary status in the sense of pixel wise segmentation. Pixels that are assigned to a defect are numbered with 1. Pixels of the defect free areas and the background are assigned to 0.

Defect detection

For quantitative evaluation of the detection results the intersection over union (IoU) was used [11]. IoU as a standard quality tool for segmentation problems and can be calculated by

$$Intersection\ over\ Union\ IoU = \frac{A \cap B}{A \cup B} \qquad (4)$$

$A \cap B$ denotes the intersection of the predicted and ground truth segmentation mask, while $A \cup B$ their union. To be recognized as correct segmentation, IoU must be greater than 0.5. In Figure 3 the calculated IoU value is indicated above each defect image. All defects could be detected very well by the trained U-Net.

Figure 3 shows the defect detection by the U-Net for selected phase images at the first analysis frequency. The ground truth of the respective defect is marked in blue color. Red color indicates the defect detected by the network.

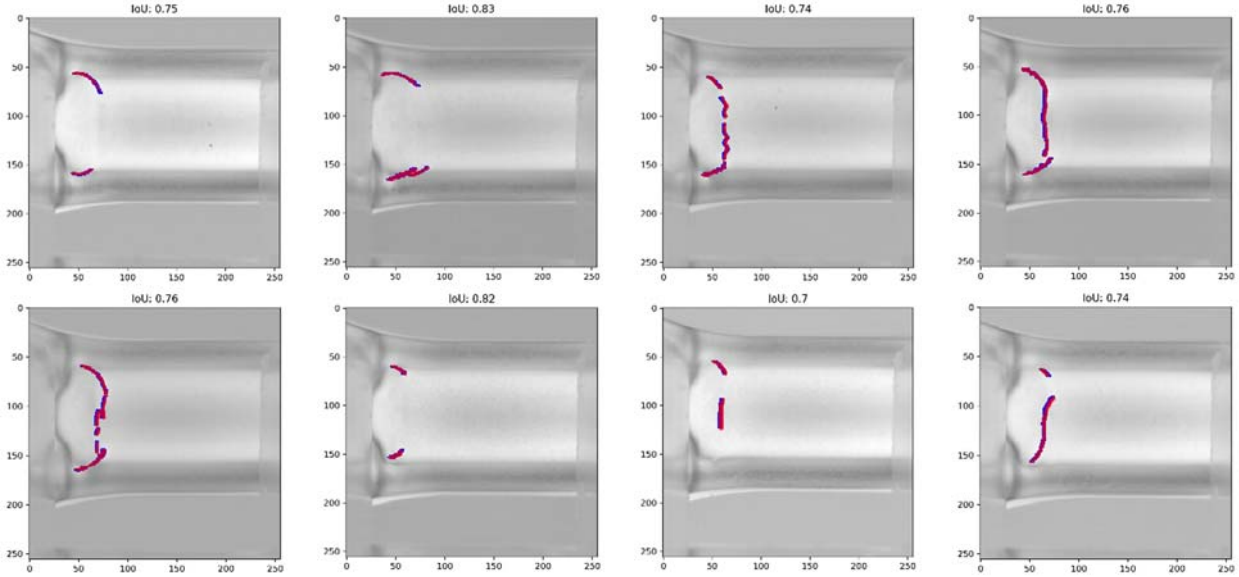

Fig. 3. *Results of the defect detection. The phase images at the first analysis frequency are overlaid with ground truth masks in blue and the predicted defect masks by the neural network in red.*

Defects were detected in excellent accordance with the result of MT testing. There were no false alarms with defect-free samples. A broader study is under work.

REFERENCES

[1] Koch S. Non-destructive testing of bars by inductive heat-flux thermography, Millenium Steel India (2014), pp 140–142
[2] Srajbr C. Induktionsthermografie als Werkzeug zur automatisierten Bauteilprüfung in Laserschweißprozessen, Thermographie-Kolloquium, Halle 2019
[3] Netzelmann U, Walle G, Lugin S, Ehlen A, Bessert S and Valeske B. Induction thermography: principle, applications and first steps towards standardization, QIRT Journal (2016)
[4] Sakagami T, Ogura K. Thermographic NDT based on transient temperature field under Joule effect heating, Thermosense XVI, SPIE 2245 (1994) 120-130
[5] Valeske B, Bessert S, Walle G und Netzelmann U. Qualifizierung und Validierung der induktiv angeregten Thermographie für die Oberflächenrissprüfung von metallischen Bauteilen, Thermographie Kolloquium 2009, 8.-9.10.09, Stuttgart, DGZfP Berichtsband BB 119-CD, P01 (2009)
[6] Walle G, Netzelmann U, Stumm C and Valeske B. Low frequency induction thermography for the characterization of hidden cracks in ferromagnetic steel components, Proc. 11th Int. Conf. on Quantitative Infrared Thermography (QIRT), 11.-14.6.2012, Naples, Italy, paper 218
[7] Thiemann C, Zaeh M, Srajbr C and Böhm S. Automated defect detection in large-scale bonded parts by active thermography, Proc. 10th Int. Conf. on Quantitative Infrared Thermography, July 27-30, Quebec, Canada
[8] Oswald-Tranta B, Schmidt R. Crack depth determination with inductive thermography, Proc. SPIE Sensing Technology (2015)
[9] Ronneberger O, Fischer P, Brox T. U-Net: Convolutional Networks for Biomedical Image Segmentation Medical Image Computing and Computer-Assisted Intervention (MICCAI), Springer, LNCS, Vol.9351: 234--241, 2015
[10] Maldague X. Theory and Practice of Infrared Technology for Non-Destructive Testing. John Wiley & Sons, 2001, Chapter 6
[11] Everingham M, Eslami S.M.A., Van Gool L. The Pascal Visual Object Classes Challenge: A Retrospective, Int J Comput Vis 111, 98–136 (2015)